

Fine-Grained Fusion: The Missing Piece in Area-Efficient State Space Model Acceleration

Robin Geens*
robin.geens@kuleuven.be
MICAS, KU Leuven
Leuven, Belgium

Arne Symons*
arne.symons@kuleuven.be
MICAS, KU Leuven
Leuven, Belgium

Marian Verhelst
marian.verhelst@kuleuven.be
MICAS, KU Leuven
Leuven, Belgium

ABSTRACT

State Space Models (SSMs) offer a promising alternative to transformers for long-sequence processing. However, their efficiency remains hindered by memory-bound operations, particularly in the prefill stage. While MARCA, a recent first effort to accelerate SSMs through a dedicated hardware accelerator, achieves great speedup over high-end GPUs, an analysis into the broader accelerator design space is lacking. This work systematically analyzes SSM acceleration opportunities both from the scheduling perspective through fine-grained operator fusion and the hardware perspective through design space exploration, using an extended version of the Stream modeling framework.

Our results demonstrate that the improved data locality stemming from our optimized fusion and scheduling strategy enables a speedup of up to 4.8 \times over unfused execution, while our adaptive memory-aware fusion approach reduces on-chip memory requirements by an order of magnitude without sacrificing performance. We further explore accelerator design trade-offs, showing that a fusion-aware hardware architecture can achieve 1.78 \times higher performance than the state-of-the-art MARCA accelerator, within the same area budget. These results establish operator fusion as a key enabler for next-generation SSM accelerators.

KEYWORDS

State Space Models, Design Space Exploration, Operator Fusion, Hardware Efficiency, Accelerators

1 INTRODUCTION

Large Language Models (LLMs) with transformer-based architectures [23] have revolutionized applications ranging from natural language processing to multimodal applications. Despite their immense success, deploying these models presents significant challenges due to 1) their enormous size, often exceeding a billion parameters, and 2) the quadratic computational and memory scaling of their self-attention mechanisms, which hinders the processing of long input sequences. Techniques such as caching, quantization, sparsity exploitation, and optimized dataflows [10, 16] help mitigate these issues, but deployment challenges persist, particularly in resource-constrained environments and for long sequences.

State Space Models (SSMs) [4, 5, 7] have emerged as a compelling alternative to transformers, offering linear computational complexity and constant memory scaling relative to sequence length. Figure 1 highlights this distinction by comparing computation and memory characteristics of transformers (OPT-2.7B [27]) and SSMs (Mamba-2.8B [4]) in two key processing stages. During the *prefill*

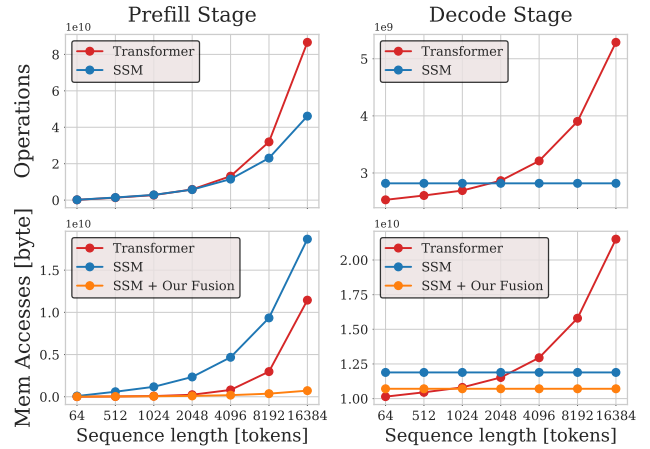


Figure 1: Comparison of transformer-based OPT-2.7B and SSM-based Mamba-2.8B during inference for the prefill stage (left) and decode stage (right). SSMs exhibit constant operations and memory usage during the decode stage, whereas the prefill stage presents a trade-off: lower operations but higher memory requirements compared to transformers.

stage, when the model processes the initial input sequence before generating new tokens, SSMs require more frequent memory accesses compared to transformers, which poses challenges for efficient hardware acceleration. In contrast, during the *decode stage*, where new tokens are generated sequentially, transformers rely on retrieving previously processed tokens from a key-value (KV) cache, while SSMs update a compact internal state instead. This gives SSMs a significant advantage for long sequences, reducing memory overhead and improving scalability.

MARCA [13] represents the first effort towards dedicated hardware acceleration of SSMs, achieving up to 11 \times speedup over a high-end GPU by employing highly-parallel reconfigurable processing elements. However, MARCA does not explore the impact of the number of parallel compute elements or the size of its embedded memory, presenting only a single design of an accelerator with a fixed area ratio of compute units to memory resources. The lack of a comprehensive analysis on the optimal hardware architecture configuration underlines the need for broader studies into SSM accelerator design, aiming to further enhance the performance of hardware accelerators for different use cases.

To address these challenges, this work comprehensively examines the computational characteristics of SSMs on dedicated hardware accelerators in order to provide broadly applicable insights. Our contributions are shown in Figure 2 and summarized as follows:

*Equal contribution

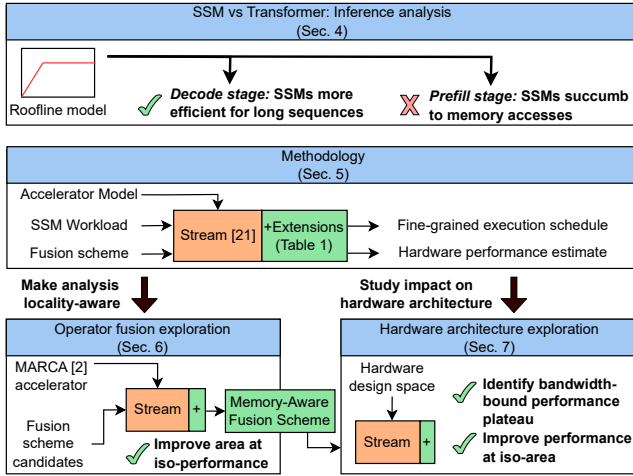


Figure 2: Overview of this paper.

- A high-level roofline analysis across transformers and SSMs, identifying the critical need for enhanced on-chip data reuse of SSMs during the prefill phase (Section 4).
- Open-source extensions to the Stream modeling framework to enable precise performance estimation and automatic scheduling for SSM accelerators with optimized data locality (Section 5).
- Development of an advanced operator fusion and scheduling strategy that can improve performance by as much as $4.8\times$ (Section 6).
- Exploration of the hardware accelerator design space showing that 1) identical performance constraints can be met while reducing the on-chip memory area by an order of magnitude, or 2) performance can be boosted by $1.78\times$ under iso-area constraints compared to a state-of-the-art of SSM accelerator MARCA (Section 7).

2 BACKGROUND

2.1 LLM Inference Stages

Large Language Models (LLMs) are deep neural networks—often consisting of hundreds of millions to hundreds of billions of parameters—that are trained on vast corpora of text data. During inference, LLMs generate new text predictions from a given prompt or input context. Inference commonly involves two distinct computational stages: *prefill* and *decode*. During the prefill stage, the model processes the entire input sequence in one forward pass, computing sequence transformations that encode contextual relationships. In the subsequent decode stage, outputs are generated autoregressively, one token at a time.

2.2 The Dominance of Transformer-based LLMs

Transformer-based LLMs [23] have become fundamental to modern AI applications. Their effectiveness largely stems from the self-attention mechanism that captures pairwise dependencies across tokens in an input sequence. However, this comes with a significant computational cost: during the *prefill phase* self-attention operations scale as $O(L^2)$ in time and in memory usage. This makes transformers particularly inefficient for long-sequence processing.

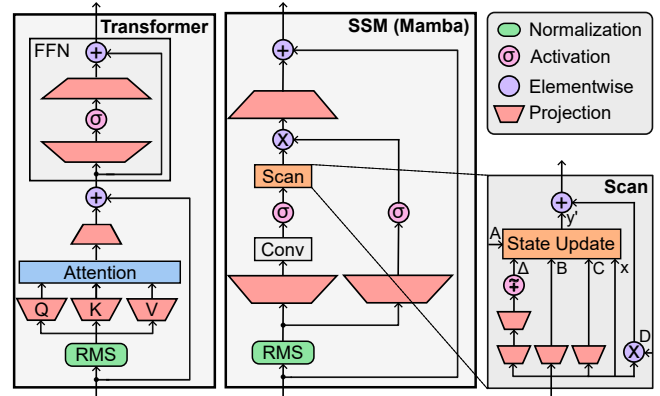


Figure 3: Architecture overview of transformers and SSMs. The state update block is detailed in Figure 7.

2.2.1 Key Operations. The computational workload of transformer models is dominated by two main types of operations, as illustrated on the left side of Figure 3:

Attention. The attention mechanism involves matrix multiplications to compute query-key similarity scores, followed by a softmax operation and matrix multiplication with value vectors to generate outputs. These operations collectively form the computational backbone of transformers, with the $O(L^2)$ complexity arising from the computation of pairwise token interactions. Additionally, the softmax operation contains multiple non-linear operators and requires multiple passes over the input sequence, further increasing the implementation complexity.

Projection. Projection operators are fully connected layers and are used to compute the Q , K , V and attention output matrices, as well as in the feedforward network (FFN). These operators contain model weights that define the linear projection from the operator’s input space to the output space. The weights of all projection layers collectively make up the transformer model’s parameter count.

2.2.2 Models. Transformer-based LLMs have seen widespread development, with numerous models optimized for different use cases. One widely used model family in academic research is OPT [27], valued for its open-source availability and efficient scaling, making it a strong benchmark for studying transformer architectures. Other notable model families include GPT [18], known for its strong reasoning capabilities, and the open-source LLaMA [22], which prioritizes deployment efficiency.

2.2.3 Dedicated Accelerators. In recent years, numerous hardware accelerators for transformer-based LLMs have been published [1, 8, 11, 12, 14, 19, 20, 25, 28]. These accelerators mainly target the prefill stage and employ custom techniques to exploit quantization or sparsity.

2.3 State Space Models: A Promising Alternative

State Space Models (SSMs) transform sequences by leveraging hidden state updates to retain past token information. Unlike recurrent neural networks (RNNs), which lack parallelized training, SSMs support efficient parallelization during training while maintaining

sequential dependency modeling. At inference, they achieve $O(L)$ (linear) computation and $O(1)$ memory usage complexity.

2.3.1 Key Operations. The computational foundation of SSMs lies in the efficient use of the structured linear and elementwise transformations of a state-space representation. Figure 3 (right) shows the model architecture of Mamba [4], a popular SSM. Key operations include:

State Update. SSMs maintain a hidden state h that serves as memory to process sequential data. In modern architectures such as Mamba, the state evolves through input-dependent transformation matrices, enabling dynamic updates. These updates involve multiple matrix-matrix multiplications, where the D -dimensional input is expanded by a factor N : the state dimension. The input x is transformed with the input-dependent matrices after discretization (denoted as \bar{A} , \bar{B} , and \bar{D}) to produce an updated state and output y :

$$\begin{aligned} h_t &= \bar{A}h_{t-1} + \bar{B}x_t \\ y_t &= Ch_t + \bar{D}x_t \end{aligned} \quad (1)$$

One key characteristic of SSMs, and a popular argument to favor SSMs over more traditional RNNs, is the potential use of a parallel scan (pscan) algorithm [15]. The pscan algorithm updates the internal state in a parallel manner instead of a purely sequential one [6]. This technique greatly speeds up training and inference time on GPUs by utilizing multiple hardware resources concurrently and eliminating sequential dependencies.

Projection. The input is projected into a higher-dimensional D space using input transformation matrices, while the output sequence is reconstructed through output transformation matrices.

Elementwise Operations. Elementwise operations, such as multiplications and residual additions, are computationally lightweight but lack data reuse, leading to inefficient memory access patterns. Despite their simplicity, their minimal data reuse can become a performance bottleneck, especially in bandwidth-limited hardware.

2.3.2 Models. Early work on linear state spaces demonstrated the feasibility of representing sequences with structured time-invariant systems [7]. Later, S4 [5] introduced parameter-efficient techniques to capture long-range dependencies, leveraging advanced initialization and diagonal state representations to rival transformers. Building on these ideas, Mamba [4] further refined SSMs by introducing selective state spaces, optimizing different regions of the state for improved accuracy and computational efficiency. This has positioned Mamba as a strong competitor to transformers, particularly for long-sequence processing. Notably, it has been shown that Mamba achieves similar accuracy to the state-of-the-art transformer models when matched for parameter count, highlighting its potential as an efficient alternative [4].

A recent trend in LLM development is the emergence of hybrid transformer-SSM architectures that aim to leverage the strengths of both approaches. SSMs efficiently track long-term information in a more diffuse manner, akin to how humans recall the general atmosphere of past events, while transformers excel at retrieving precise details (like names or addresses). Notable examples include Zamba [3], which stacks SSM and transformer layers sequentially, and Hymba [2], which integrates both mechanisms within each layer by combining transformer and SSM heads in parallel. While

this work primarily focuses on SSM acceleration, the presented techniques can also be applied to the SSM components of hybrid models.

2.3.3 Dedicated Accelerators. To the best of our knowledge, MARCA is the first and currently the only dedicated Mamba accelerator, designed for cloud environments. This architecture comprises 8192 processing elements (PEs), 24 MiB of on-chip SRAM, and 256 GB of off-chip memory bandwidth, operating at 1 GHz. This results in a design where 80 % of the area is allocated to memory resources, leaving 20 % for compute units.

Unlike traditional accelerators that rely on specialized functional units, MARCA employs flexible PEs capable of executing all required operations, including complex non-linear functions. This eliminates the need for separate functional units or vector arrays, minimizing area overhead. While certain operations require multiple cycles, they are still handled efficiently within the parallel PE arrays, maintaining computational versatility without additional architectural complexity.

2.4 Operator Tiling and Fusion

Operator tiling optimizes on-chip data locality by restructuring loop-based computations to reduce data movement. For operators expressible as Einsums or nested loops, tiling partitions loop dimensions into outer and inner loops, ensuring that inner loops execute entirely within on-chip memory. This minimizes costly memory transfers, leading to improved performance. We define a *tile* as the computation of all inner loops within a single outer loop iteration, while the *number of tiles* corresponds to the total outer loop iterations required to process the full workload.

Operator fusion further enhances data locality by executing multiple operators consecutively while keeping intermediate results on-chip. A common example is fusing activation functions with preceding layers. Fusion is closely associated with tiling, where computations are first divided into tiles that fit within on-chip memory and then executed in a fused manner. For example, if two fused operators each have n tiles, the execution proceeds in n iterations, with each iteration processing the corresponding tiles from both operators in sequence. However, fusion requires knowledge of data dependencies between tiles, which is not always straightforward when intermediate tiles undergo complex transformations.

For transformer models, operator fusion is well-studied. Notably, FuseMax [16] optimizes softmax computation by reducing the number of memory accesses and redundant passes over the sequence. FLAT [10] improves on this work and fuses attention score computation, softmax normalization, and key-value weighting into a single operation, minimizing memory bandwidth requirements. However, for SSMs models, operator fusion studies are missing, aside from some GPU inference optimizations proposed by the author of Mamba [4].

2.5 Stream Framework for Accelerator Modeling and Operator Fusion

Stream [21] is a modeling and scheduling framework that estimates and optimizes the performance of multi-core dataflow accelerators. Given an accelerator hardware architecture and a target neural network model for deployment, it models the on-chip dataflow,

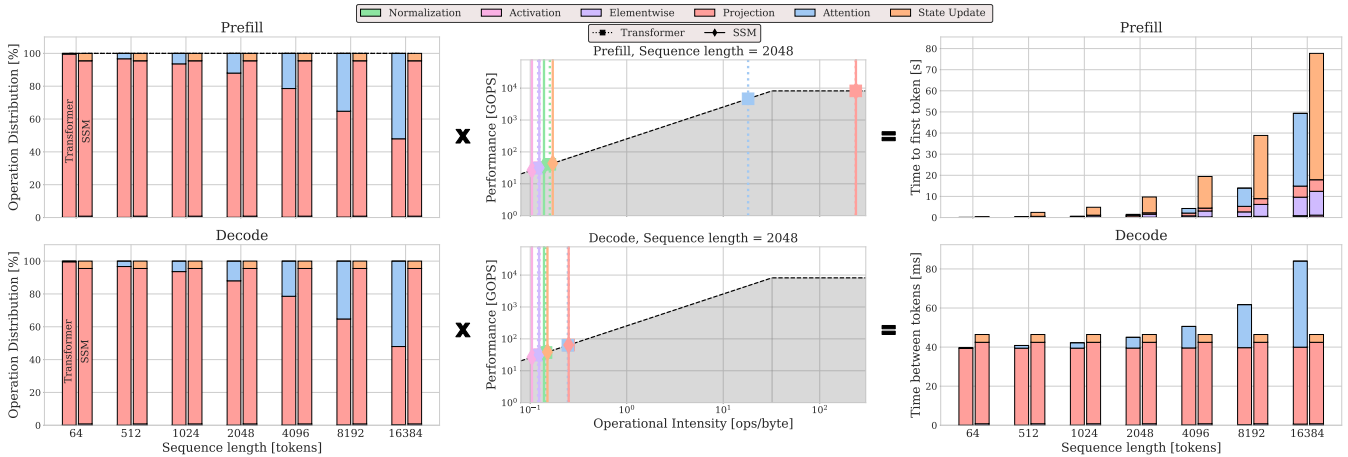


Figure 4: Inference latency (right) for the OPT-2.7B transformer (left bars, squares) and the Mamba-2.8B SSM (right bars, diamonds) across stages and sequence lengths. Operator distribution (left) and intensity (middle) shape the total latency. The roofline is shown for the $L = 2048$ case. SSMs perform worse in the prefill stage due to memory-bound state-update operators.

on-chip memory and core interconnection pattern with limited bandwidth to derive an optimized execution schedule and energy and latency predictions. Accurate performance estimation is obtained through a memory manager and a communication manager. The memory manager tracks the movement and storage of tensors, prioritizing on-chip data locality. The communication manager provides estimates of communication overheads for the required tensor transfers between cores. Stream supports a variable computation granularity—from coarse operator-by-operator processing to fine-grained operator fusion—and schedules all tiles with an adaptable scheduling order. This makes it a versatile tool for exploring both the fusion and accelerator design space. However, while Stream supports a wide range of different workloads through an ONNX [17] front-end, there are key aspects missing for modeling LLMs.

3 MOTIVATION, CHALLENGES & GOALS

3.1 Motivation

Efficient LLM inference is critical for many applications, particularly in real-time or autonomous systems that demand low-latency execution. Custom hardware accelerators have played a key role in optimizing efficiency for domain-specific workloads, particularly in deep learning. While numerous accelerators have been proposed for transformer-based LLMs, far fewer exist for SSM-based models, despite their promising efficiency in long-sequence processing.

However, developing specialized accelerators is a long and costly process. Hardware design cycles can take months, making it essential to gain early insights into viable accelerator architectures.

3.2 Challenges

We identify three key challenges for efficient LLM hardware acceleration:

Computational Complexity. LLMs require extensive computation and data movement. However, the workload characteristics vary drastically depending on the use case, such as inference stages (prefill, decode) and sequence length. It is unclear which LLM architecture performs best when different scenarios are considered,

as demonstrated in Figure 1. A deep understanding of operator types and their behavior on accelerators is necessary to optimize inference performance.

Operator Fusion. Reducing data movement through operator fusion has been widely studied for transformer-based models [10, 16]. However, the potential for operator fusion in SSMs remains largely unexplored. Understanding which SSM operators can be fused, what tile sizes are optimal, and how this impacts hardware performance is essential for improving efficiency.

Rapid Hardware DSE. LLM architectures evolve rapidly, making it crucial to assess their impact on accelerator performance early. Key hardware components—including compute resources, dataflow, memory capacity, and off-chip bandwidth—all influence cost and performance. MARCA [13], a state-of-the-art SSM accelerator, provides insights into one specific design point but does not explore the broader design space. Traditionally, evaluating different architectural configurations requires multiple low-level hardware implementation iterations, each taking weeks, while cycle-accurate simulations of LLM models with high parameter counts further slow down exploration by requiring days per evaluation. Faster evaluation methods are needed to efficiently analyze the design space and guide architectural decisions beyond a single accelerator instance.

3.3 Goals

The goals of this paper link to the three challenges:

Computational Complexity. Analyze the operator distribution in transformer- and SSM-based LLMs and perform a high-level performance analysis across different use cases.

Operator Fusion. Explore new fusion and scheduling strategies to optimize on-chip data reuse and efficiently accelerate SSM models.

Rapid Hardware DSE. Evaluate how hardware architecture decisions impact SSM inference performance, incorporating optimized fusion strategies to come to improved accelerator architectures.

4 TRANSFORMER vs. SSM ANALYSIS

Figure 1 summarizes the total operations and memory accesses required for inference across different stages (prefill and decode) of transformer- and SSM-based LLMs, providing proxy metrics for performance. Throughout this paper, we use OPT-2.7B [26] as the representative transformer model and Mamba-2.8B [4] as the SSM model. These models are well-matched in terms of parameter count and accuracy [4], making them a fair basis for comparison. However, the total number of operations alone does not fully capture latency bottlenecks, as different operator types contribute unequally to execution time.

4.1 Operation Distribution

To better understand the unequal contribution of operator types to the total latency, Figure 4 (left) shows the distribution of the number of operations across different operator types for transformers (left bars) and SSMs (right bars). Notably, these distributions remain nearly identical between the prefill and decode stages. For transformers, this is due to KV caching, which reduces both projection and attention computations proportionally. For SSMs, the distribution remains unchanged across stages and sequence lengths due to their recurrent formulation, where structured state-space updates and projections are applied uniformly at each step.

Among all operator types, projections account for the largest share of operations, except in transformers at large sequence lengths, where attention begins to dominate due to the quadratic scaling of query-key interactions.

4.2 Operational Intensity

The latency cost of operator types is heavily influenced by their *operational intensity* (OI), defined as the ratio of operations to memory accesses (in operations per byte). A higher OI indicates better data locality (cfr. Section 2.4), as more computations are performed per byte transferred from memory. The x-axis of Figure 4 (middle) illustrates the OI of different operator types in transformers (dashed lines, squares) and SSMs (full lines, diamonds).

In the prefill stage, projection operators of both transformers and SSMs exhibit the highest OI due to their large matrix-matrix multiplications, which enable significant data reuse. Transformer attention also exhibits high OI , as the query-key multiplication operates on the entire sequence at once, leading to substantial reuse of key and query activations. This results in an OI of 18.1 ops/byte. In contrast, SSM state updates apply structured recursions on a single token at a time, preventing any substantial reuse across the sequence. As a result, their OI is significantly lower at just 0.17 ops/byte.

In the decode stage, OI drops significantly across all operators. Unlike in the prefill phase, where computation on the entire sequence enables data reuse, the decode stage operates autoregressively, processing one token at a time. This severely limits data locality, forcing frequent memory accesses for each new token. As a result, even projection operations, which were previously compute-bound, shift toward a memory-bound regime. This fundamental characteristic impacts both transformers and SSMs.

4.3 Roofline Model Performance

The *hardware roofline model* provides an intuitive framework to analyze the performance of different operators (characterized by their OI), relative to the hardware specifications in terms of off-chip bandwidth and peak computational performance [24], and identifies memory-bound and compute-bound regions.

Figure 4 (middle) presents the roofline plot for the MARCA accelerator with its $P_{\text{peak}} = 8192 \text{ GOPS}$ and $BW = 256 \text{ GB/s}$. We superimpose its impact on transformer and SSM-based models for a sequence length of 2048 tokens. The performance of each operator type is computed based on its OI and the hardware constraints. As expected, projection operators fall in the compute-bound region due to their high reuse. Meanwhile, all other operators, including attention and SSM state updates, remain memory-bound. Despite both being memory-bound, attention achieves a performance of 4633 GOPS , compared to the SSM state-update 44 GOPS , a performance reduction of more than 100 \times .

4.4 Latency Implications

To approximate inference latency, we combine operation counts with the operational intensity (OI) of each operator. This estimate assumes a conventional layer-by-layer execution model, without leveraging operator tiling or fusion optimizations. Figure 4 (right) illustrates the absolute latency for both models. For the prefill stage, latency corresponds to the time required to generate the first token (measured in seconds, shown at the top). In the decode stage, it represents the time between consecutive token generations (measured in milliseconds, shown at the bottom).

4.4.1 Prefill Stage. Although projection operators dominate the operation count, their high OI ensures they have minimal impact on latency. The latency of the transformer scales roughly quadratically with sequence length due to the quadratic growth of attention operations, while the SSM’s latency increases linearly. However, despite its favorable scaling, the SSM exhibits consistently higher latency than the transformer across all sequence lengths. This is primarily due to the memory-bound SSM state update operations that suffer from an OI approximately 100 \times lower than the attention of the transformer.

Takeaway 1. The SSM’s latency is dominated by state update operations with 100 \times lower OI compared to transformer’s attention operators. By increasing the OI of these operators through data reuse optimizations, we can further reduce the total latency. In the next section, we explore how operator fusion can be leveraged to achieve this improvement.

4.4.2 Decode Stage. In the decode stage, the SSM maintains constant latency across sequence lengths due to the fixed size of its internal state. For short sequences, it is slower than the transformer because of a large state expansion factor. However, its latency is dominated by projection operators, which are relatively slow. In contrast, the transformer’s latency increases with sequence length because attention operations scale linearly in this stage.¹ Consequently, for long sequences, the SSM is significantly faster, as intended by design.

¹Attention grows linearly, not quadratically, with sequence length in the decode stage since only a single token is generated at a time.

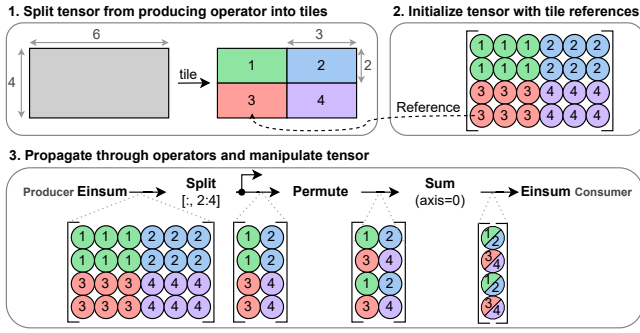


Figure 5: Dependency tracking using emulation of complex tensor manipulations between a *producing* and *consuming* operator. At the end, the exact dependencies for every individual element in the consuming operator’s input are known.

Takeaway 2. In the decode stage, SSM latency is fundamentally constrained by the dominance of projection operators and memory bottleneck. Further latency reductions would require either increased bandwidth, reduced bitwidth of the projection weights, or alternative accelerator technologies, such as digital in-memory computing.

5 METHODOLOGY

This section presents the main methodology used throughout the rest of this paper, as illustrated in Figure 2. At its core, we employ Stream [21], a versatile performance estimation framework capable of tracking memory contents over time.

While the roofline analysis offers high-level insights into computational bottlenecks and memory-boundedness, it does not capture on-chip data locality across operators or account for resource utilization. By leveraging Stream, we overcome these limitations, enabling a more detailed investigation of on-chip memory utilization, tiling, and fusion strategies. This analysis is particularly crucial during the prefill phase of SSM execution, where efficient memory access patterns play a key role in overall performance.

Section 5.1 proposes the open-source extensions to Stream that enable flexible tiling of multiple SSM operators, accurate identification of inter-tile dependencies, and efficient scheduling of fused tiles. Next, the precise setup and major inputs to Stream are specified: Section 5.2 details how the SSMs are translated to ONNX format and Section 5.3 defines the high-level hardware accelerator model used throughout the further explorations and optimizations of this paper.

5.1 Extending Stream for Dependency-Oriented Analysis

To accurately represent SSM workloads and track dependencies between fused tiles, we introduce several modifications to the Stream framework. The extensions, summarized in Table 1 and detailed next, will be made available as open-source contributions.

5.1.1 Operator Support. While Stream accepts ONNX models as workload inputs, standard ONNX operators are insufficient to represent the state update mechanism of SSMs due to its recurrent nature. To address this limitation, we extend the ONNX operator

Table 1: Our extensions to Stream framework

	Stream [21]	Ours
Operator Support	GeMM, Conv, Elementwise	+Einsum, Softmax, External product, Reduction
SSM State Update	✗	✓
Dependency Tracking	R-tree	Tensor-based (Fig. 5)
Multi-cycle Operators	✗	✓

set with a custom SSM operator and modify Stream’s ONNX parser to correctly interpret this operator. The parser decomposes the SSM operator into atomic operations, while also ensuring proper handling of dependencies between the atomic operations, and between prior operators and the state update block. The implementation of the state update is later detailed in Section 5.2.

Other SSM that were not yet supported by Stream’s ONNX parser, such as Einsum operations, external products, and reduction operations (e.g., the sum over a given axis), are also added.

5.1.2 Dependency Tracking. We propose a novel dependency tracking mechanism that efficiently and accurately infers all inter-tile dependencies, regardless of the tiling and fusion strategy. The existing Rtree-based dependency tracking in Stream is limited to cases where producer and consumer tiles have matching dimensions. However, SSMs frequently employ operators such as Split, Slice, and Transpose, that alter the tensor dimensions between the producer and consumer tiles. To accommodate these transformations, a more general dependency tracking mechanism is required.

To address this challenge, we introduce a tensor-based approach that tracks dependencies at element granularity, as summarized in Figure 5. In this method, the output of each (untiled) operator is represented as a tensor, where each element references the tile that produced it. These dependency-tracking tensors enable arbitrary tiling strategies as specified by the user. They are then propagated through the complex operators, accurately reflecting operations that modify the shape, order, or structure of elements. Additionally, we introduce heuristics to identify tensor dimensions unaffected by specific transformations and exclude them from dependency tracking, thereby reducing unnecessary computations.

5.1.3 Multi-cycle Operators. Beyond the standard MAC operations, SSMs incorporate operators that may require multiple cycles per operation when executed on hardware accelerators, such as exponentiation and activation functions. This characteristic affects achievable performance, potentially increasing latency in compute-bound scenarios while having minimal impact on memory-bound computations. To accurately capture this effect, we extend Stream to allow users to specify cycle-per-operation (CPO) characteristics for individual operators.

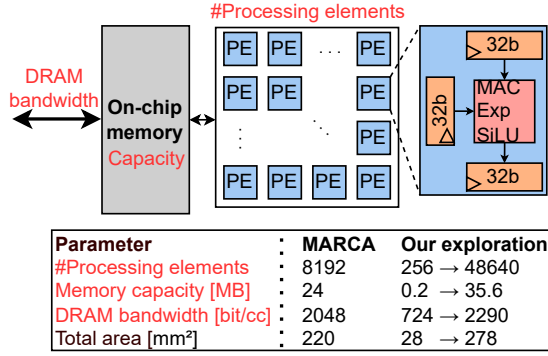


Figure 6: Diagram of the parameterized accelerator model, with parameter values for MARCA and our hardware design space exploration (Sec. 7).

5.2 Workload model

Stream accepts an ONNX [17] graph as input to represent workloads. The full SSM shown in Figure 3 is first implemented in PyTorch and then exported to ONNX. By leveraging our extensions to the ONNX parser, Stream can correctly interpret all SSM operations.

As mentioned in Section 2, the state update block is typically implemented using a pscan algorithm. However, in this work, we opt for a purely sequential implementation for three reasons: 1) Dataflow architectures with 2D PE arrays do not benefit as much from pscan as the streaming multiprocessors found in GPUs. 2) pscan necessitates batched execution for large sequence lengths due to its substantial memory requirements. 3) pscan has a higher time complexity of $O(L \log_2 L)$ [9], whereas the sequential implementation has a linear complexity of $O(L)$.

The decomposition of the sequential state update block is illustrated in Figure 7. In this implementation, the Δ , B and x tensors are first processed for all timesteps simultaneously, yielding the tensors $Exp(A)$ and ΔBx . The state h is then updated sequentially for each timestep, starting from the initial state h_0 . At each timestep, only a single slice of the $Exp(A)$ and ΔBx tensors is used, extracted by indexing the L dimension with the timestep index. At any given time, only one intermediate version of the state is stored, yet all y' tensors (one per timestep) are retained for later use.

5.3 Hardware Model

Stream requires a high-level description of the target hardware accelerator as input. In this abstraction, an accelerator consists of multiple cores connected via a user-defined interconnect topology, where each link is characterized by its bandwidth and energy cost. A core may represent either a computational unit, defined by its on-chip memory hierarchy and processing element (PE) array dataflow, or a memory unit such as off-chip working memory. This flexible representation enables the modeling of heterogeneous architectures with diverse core configurations.

For our analysis, we explore SSM-specific accelerators in Stream starting from MARCA [13]. Figure 6 illustrates the accelerator template alongside the parameter values used to model MARCA, as well as the parameter ranges explored in Section 7. In correspondence with MARCA’s PE design, we set the CPO of exponentiation,

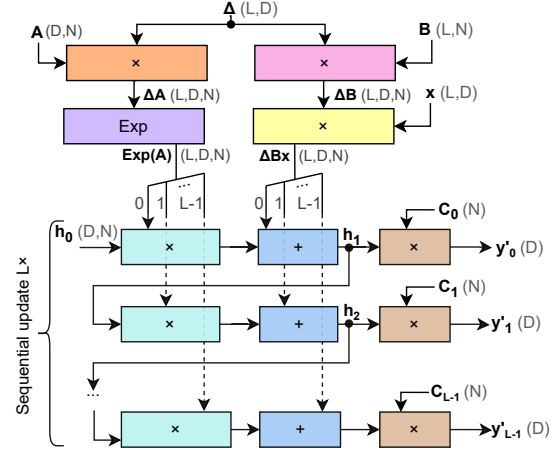


Figure 7: Diagram of the sequential state update block for L timesteps. Tensor names are in bold.

SiLU and sigmoid operations to 4. Given that our primary focus is the impact of on-chip data locality through operator fusion on overall latency, we assume a sufficiently high on-chip memory bandwidth to prevent computational stalls in the PE array. This assumption is reasonable for accelerators, as their PE arrays and memory hierarchies are typically co-optimized. To further expedite simulations, MARCA’s 32 tensor cores are aggregated into a single core with 8192 PEs, while still accounting for potential spatial under-utilization. These specifications align with contemporary accelerator designs, providing a representative framework for deriving broadly applicable insights.

For the workloads and architectures studied in this paper, the simulation time for a single design point is in the order of minutes.

6 ARCHITECTURE- & FUSION-AWARE ANALYSIS

In this section, we leverage Stream to explore various operator fusion strategies aimed at improving on-chip data locality. After exploring the fusion depth in Section 6.1, we analyze the hardware implications of the most effective fusion scheme in Section 6.2, followed by further optimizations in Section 6.3.

6.1 Exploring Fusion Depth

To incorporate the inter-operator data reuse opportunities in the SSM analysis, we devise various fusion possibilities and evaluate their effect on latency. As a first step, we explore the effect of the fusion depth, defined as the number of consecutive operator tiles executed without reloading intermediate activations from off-chip memory.

We limit the fusion evaluation to operators within the SSM state update block depicted in Figure 7, as they are expected to benefit the most from operator fusion due to their low OI , as discussed in Section 4. Each fusion scheme is defined by a specific set of fused operators and corresponding on-chip tensor retention strategies.

We tile output tensors along the token dimension L , effectively splitting (L, D, N) tensors into L tiles of shape $(1, D, N)$. Tiling along the L dimension ensures compatibility with the sequential state

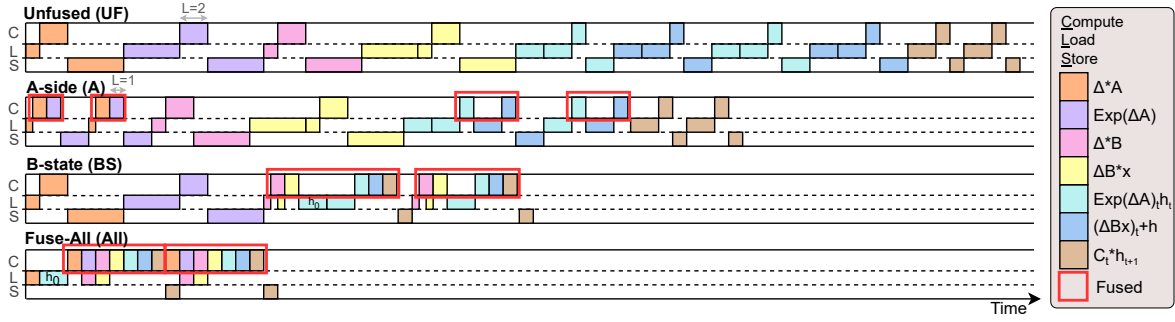


Figure 8: Execution schedule of different fusion schemes. Not drawn to scale.

update and identical performance independent of sequence length. In contrast, tiling along the D or N dimension alone would yield tensor sizes that still depend on L , potentially exceeding on-chip memory limits for long sequences and negating fusion benefits.

Table 2 summarizes all explored fusion schemes, where the number of local on-chip tensors corresponds to the fusion depth. Each listed tensor is tiled into L parts, with tiles scheduled consecutively to ensure immediate consumption by subsequent operators, preventing off-chip memory transfers. Figure 8 illustrates this process for a simplified case where $L=2$.

Figure 9 compares the estimated latency (normalized by the sequence length) and the overall hardware utilization for the entire SSM model across all fusion schemes and for different sequence lengths. Each increase in fusion depth consistently reduces latency due to reduced off-chip data transfers, with similar latency reductions observed for schemes of equal depth. The lowest latency is achieved when all state update operators are fused, eliminating all off-chip memory accesses. This scheme, denoted as Fuse-All, achieves an average speedup of 4.8 \times over unfused execution for long sequences. Under Fuse-All, the state update module reaches an average hardware utilization of 98.3% for all sequence lengths, effectively shifting from a memory-bound to a compute-bound regime.

Note that the average latency per token of inferences with $L=1$ (decode phase) is significantly higher due to memory-bound projection operators. For larger sequences ($L \geq 512$ in Figure 9), the

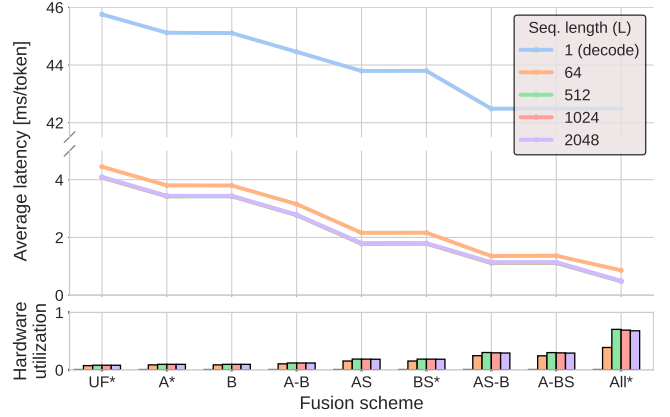


Figure 9: Evaluation of different fusion schemes using Stream. Asterisk(*) indicates fusion schemes are visualized in Figure 8.

average latency per token becomes independent of L . For these values, the projections are compute-bound, and the total latency scales linearly in L , keeping the average latency per token constant. This demonstrates that our analysis remains valid for even longer sequences.

Takeaway 3. By tiling and fusing all operators within the state update block in the L dimension, its computations shift from a memory-bound to a compute-bound regime, greatly improving performance.

6.2 Sensitivity to On-chip Memory Capacity

The Fuse-All scheme eliminates all off-chip memory transfers for the MARCA-based accelerator model with 24 MiB of on-chip memory. Next, we investigate the impact of reduced on-chip memory on performance.

The peak memory usage during fused execution can be derived analytically in terms of SSM dimension sizes. Figure 10 illustrates the tensor lifetimes for a single state update timestep under the Fuse-All scheme, with peak memory demand occurring during the computation of $Exp(\Delta A)_t \cdot h_t$. At this point, storage is required for five (D, N) -size tensors and one $(D,)$ -size tensor. Therefore, Fuse-All sets the following requirement on the on-chip memory capacity, assuming 32-bit activations:

$$|Memory| > (5DN + D) \times 32 \text{ bit} \quad (2)$$

To test this hypothesis, we gradually reduce the on-chip memory capacity of our accelerator model and estimate the inference latency

Table 2: Fusion schemes under study. Tensors are named in correspondence with Figure 7. n is computed at compile time, depending on the on-chip memory capacity.

Fusion scheme	Abbrev.	Locality of tensors	#tiles per fused layer
Unfused	UF	None	None
A-side	A	ΔA	L
B-side	B	ΔB	L
AB-sides	A-B	$\Delta A, \Delta B$	L
A-state	AS	$\Delta A, Exp(\Delta A), h (\times 2)$	L
B-state	BS	$\Delta B, \Delta Bx, h (\times 2)$	L
A-state, B	AS-B	$\Delta A, \Delta B, h (\times 2), \Delta B$	L
B-state, A	BS-A	$\Delta B, \Delta Bx, h (\times 2), \Delta A$	L
Fuse-All	All	All of the above	L
Mem-Aware	MA-All	All of the above	nL

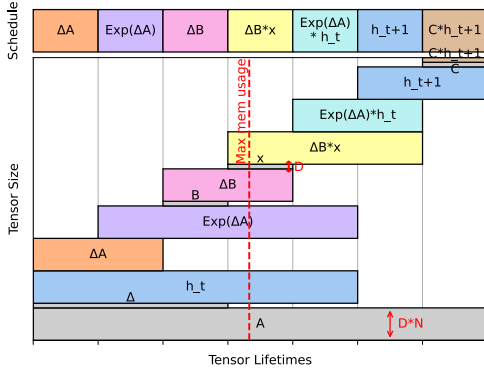


Figure 10: Schedule of operators (top) and lifetimes of tensors (bottom) of one state update iteration. A and h remain in memory throughout the entire fused execution as they are reused across iterations.

for the Fuse-All scheme, shown with full lines in Figure 11. The latency exhibits a staircase pattern, where each step corresponds to an additional off-chip transfer when an intermediate tensor no longer fits on-chip. The first major latency increase aligns with the threshold predicted by Equation (2).

Takeaway 4. Under fusion scheme Fuse-All, the on-chip memory capacity of contemporary SSM accelerator architectures can be significantly reduced without sacrificing performance, up to the threshold of Equation (2).

6.3 Memory-Aware Fusion

To enable memory-efficient inference on smaller accelerators or of SSMs with larger dimensions, we introduce a finer-grained adaptive fusion scheme: instead of solely tiling along the L dimension, activation tensors are further partitioned along the D dimension.

We choose D , as partitioning the N dimension into many small tiles would lead to spatial under-utilization of the PE array. For instance, in Mamba1-2.8B, $N=64$ while $D=5120$.

Starting from Equation (2), we determine the minimum number of splits n required in the D dimension to prevent off-chip transfers in the Fuse-All scheme, as follows:

$$n = \left\lceil \frac{(5DN + D) \times 32 \text{ bit}}{|Memory|} \right\rceil \quad (3)$$

The fusion scheme that results from tiling the fused operators in both the L dimension (L times) and D dimension (n times) is denoted as Mem-Aware. Figure 11 illustrates the performance impact of Mem-Aware fusion in function of memory capacity with dashed lines. The results demonstrate that inference latency remains stable even with a $24\times$ smaller on-chip memory. These findings suggest that large on-chip memory capacities, such as the 80% silicon area allocation of MARCA’s 222 mm^2 die, may be unnecessary for achieving optimal performance.

Takeaway 5. Under the fine-grained Mem-Aware fusion scheme, the on-chip memory capacity of contemporary SSM accelerator architectures can be reduced by an order of magnitude without sacrificing performance.

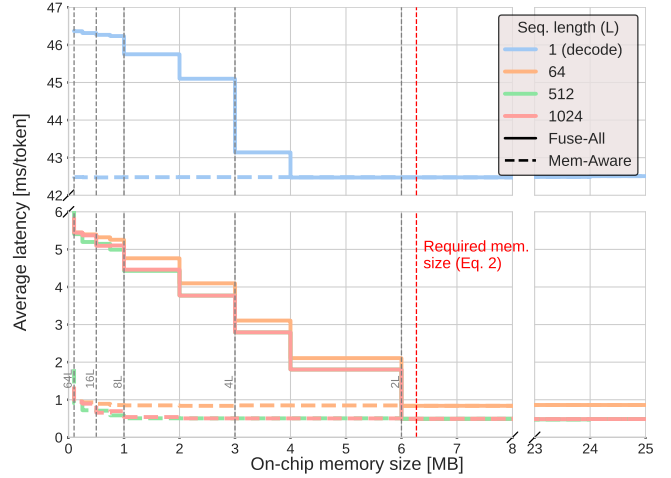


Figure 11: Sensitivity of latency to on-chip memory capacity under fusion scheme Fuse-All (full lines) and Mem-Aware (dashed lines). For Fuse-All, all fused tensor are split into L tiles. For Mem-Aware, the number of tiles per tensor is indicated next to the gray dashed lines.

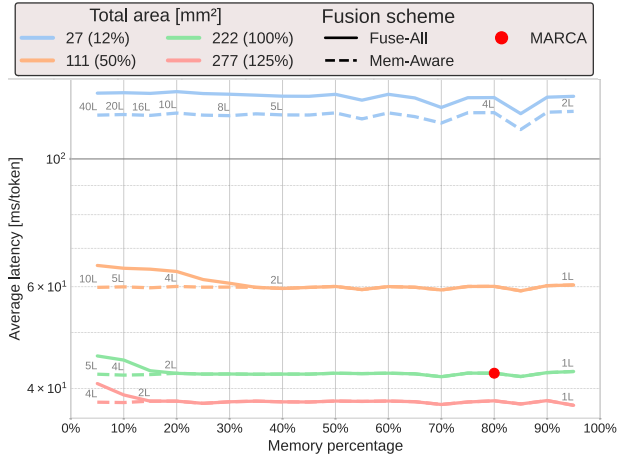
7 ARCHITECTURE DESIGN SPACE EXPLORATION

Section 6 concludes that the accelerator’s on-chip memory capacity, and consequently its area, can be substantially reduced under the same latency constraints. This finding prompts our final study: given a specific inference scenario and area budget, what constitutes an optimal SSM accelerator design, i.e. how should computational area be balanced against memory area? To answer this, we explore the accelerator design space, leveraging our enhanced version of Stream with the Mem-Aware fusion scheme to rapidly evaluate a wide variety of potential hardware configurations.

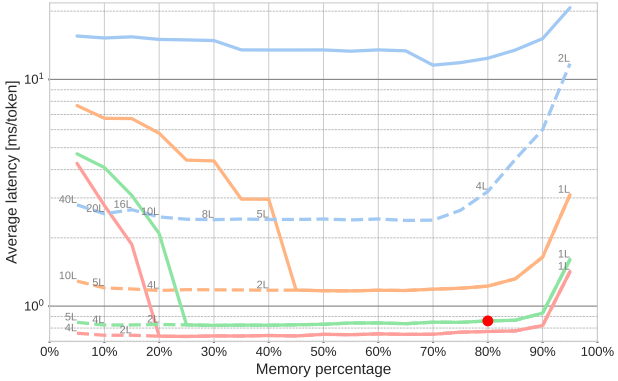
The explored design space is characterized by two primary axes: total chip area and the proportion of area allocated to memory. To traverse the first axis, the total area is varied from 12.5% to 125% of MARCA’s total area of 222 mm^2 . For the second axis, processing elements are substituted for additional memory capacity based on the relative compute/memory area costs reported for MARCA [13]. We further assume that the off-chip bandwidth scales linearly with the chip’s perimeter (commonly referred to as the *beachfront* in chiplet-based architectures), which corresponds to the square root of the total area.

Figure 12 presents the performance evaluation in the design space for the fusion schemes Fuse-All (full lines) and Mem-Aware (dashed lines), for different sequence lengths. When on-chip memory capacity is sufficiently large, the two fusion schemes exhibit identical performance, as tensors fit entirely in memory without requiring additional splits along the D dimension. However, once the memory capacity falls below the requirement established in Equation (2), the performance of Fuse-All deteriorates.

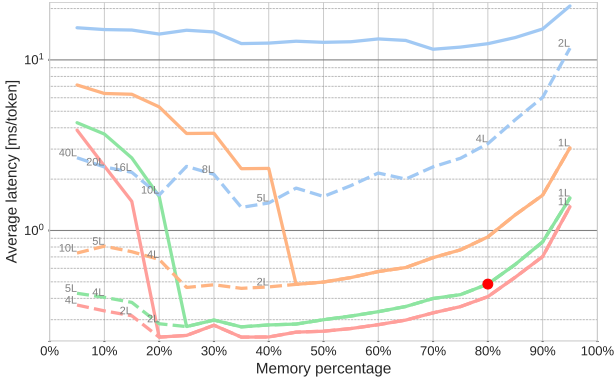
A key observation in Figures 12a ($L=1$) and 12b ($L=64$) is the presence of a broad latency plateau along the iso-area lines, rather than a sharply defined optimal point. In these cases, redistributing chip area between memory and compute units does not improve performance, as the system is constrained by off-chip bandwidth.



(a) $L=1$ (decode)



(b) $L=64$ (prefill)



(c) $L=1024$ (prefill)

Figure 12: Latency evaluations for different architecture design points. At the left-end side of the x-axis, the full area budget is spent on processing elements with no on-chip memory. Full lines represent fusion scheme Fuse-All while dashed lines represent Mem-Aware. Grey values indicate the total number of tiles per fused tensor for points on the dashed line.

The performance of these short sequence lengths is memory-bound by the projection layers, meaning that increasing neither on-chip compute nor on-chip memory capacity mitigates the bottleneck.

Takeaway 6. For small sequence lengths, where memory-bound projection operators limit the achievable performance, changing the hardware architecture (memory capacity or the total number of PEs) doesn't improve performance.

For larger sequence lengths, this off-chip bandwidth limitation diminishes, as the projection weight matrix can be reused across multiple tokens, shifting the projection layers from a memory-bound to a compute-bound regime. In Figure 12c ($L = 1024$), the set of near-optimal design points becomes significantly narrower. In particular, the MARCA architecture is positioned far from this optimal range. Under fusion scheme Fuse-All, the need for extensive on-chip memory is substantially reduced, allowing silicon area to be reallocated toward higher compute capacity. Specifically, an accelerator featuring 32,768 PEs and 10.5 MiB of SRAM would achieve a $1.78\times$ performance improvement over MARCA.

Takeaway 7. For large sequence lengths and under the Mem-Aware fusion scheme, the optimal hardware architecture configuration shifts, favoring computation units over on-chip memory and leading to a significant improvement in performance.

8 CONCLUSION

SsMs have recently emerged as a promising alternative to transformers for long-sequence processing, though efficient inference with hardware accelerators remains largely unexplored. This work demonstrated how tiling and operator fusion can transform SSM acceleration, shifting state update computations from a memory-bound to a compute-bound regime, thereby significantly improving performance. By employing an extended version of Stream, an accelerator modeling framework, we identified key data locality bottlenecks and proposed advanced fusion and scheduling strategies to mitigate them.

Our results show that our memory-aware fusion scheme enables significant reductions in on-chip memory capacity without sacrificing performance. In a hardware design exploration study, we identified that a fusion-aware SSM accelerator favors compute over on-chip memory to deliver increased throughput, compared to contemporary accelerator architectures. While the state-of-the-art MARCA accelerator provides a strong baseline, our findings highlight opportunities for further architectural improvements. These insights pave the way for more efficient hardware architectures, particularly for handling larger sequence lengths in the prefill stage.

ACKNOWLEDGMENTS

This project has been partly funded by the European Research Council (ERC) under grant agreement No. 101088865, the European Union's Horizon 2020 program under grant agreement No. 101070374, the Flanders AI Research Program, Research Foundation Flanders (FWO) under grant No. 1S37125N, and KU Leuven.

REFERENCES

- [1] Steve Dai, Hasan Genc, Rangharajan Venkatesan, and Bruce Khailany. 2023. Efficient Transformer Inference with Statically Structured Sparse Attention. In *2023 60th ACM/IEEE Design Automation Conference (DAC)*. 1–6. <https://doi.org/10.1109/DAC56929.2023.10247993>
- [2] Xin Dong, Yonggan Fu, Shizhe Diao, Wonmin Byeon, Zijia Chen, Ameya Sunil Mahabaleshwar, Shih-Yang Liu, Matthijs Van Keirsbilck, Min-Hung Chen, Yoshi Suhara, Yingyan Lin, Jan Kautz, and Pavlo Molchanov. 2024. Hymba: A

- Hybrid-head Architecture for Small Language Models. arXiv:2411.13676 (Nov. 2024). <https://doi.org/10.48550/arXiv.2411.13676> arXiv:2411.13676 [cs].
- [3] Paolo Glorioso, Quentin Anthony, Yuri Tokpanov, James Whittington, Jonathan Pilault, Adam Ibrahim, and Beren Millidge. 2024. Zamba: A Compact 7B SSM Hybrid Model. arXiv:2405.16712 (May 2024). <https://doi.org/10.48550/arXiv.2405.16712> [cs].
 - [4] Albert Gu and Tri Dao. 2024. Mamba: Linear-Time Sequence Modeling with Selective State Spaces. arXiv:2312.00752 (May 2024). <https://doi.org/10.48550/arXiv.2312.00752> [cs].
 - [5] Albert Gu, Karan Goel, and Christopher Ré. 2021. Efficiently modeling long sequences with structured state spaces. *arXiv preprint arXiv:2111.00396* (2021).
 - [6] Albert Gu, Karan Goel, and Christopher Ré. 2022. Efficiently Modeling Long Sequences with Structured State Spaces. arXiv:2111.00396 (Aug. 2022). <https://doi.org/10.48550/arXiv.2111.00396> arXiv:2111.00396 [cs].
 - [7] Albert Gu, Isys Johnson, Karan Goel, Khaled Saab, Tri Dao, Atri Rudra, and Christopher Ré. 2021. Combining recurrent, convolutional, and continuous-time models with linear state space layers. *Advances in neural information processing systems* 34 (2021), 572–585.
 - [8] Tae Jun Ham, Yejin Lee, Seong Hoon Seo, Soosung Kim, Hyunji Choi, Sung Jun Jung, and Jae W. Lee. 2021. ELSA: Hardware-Software Co-design for Efficient, Lightweight Self-Attention Mechanism in Neural Networks. In *2021 ACM/IEEE 48th Annual International Symposium on Computer Architecture (ISCA)*. IEEE, Valencia, Spain, 692–705. <https://doi.org/10.1109/ISCA52012.2021.00060>
 - [9] Mark Harris, Shubhabrata Sengupta, and John D. Owens. [n.d.]. Chapter 39. Parallel Prefix Sum (Scan) with CUDA. <https://developer.nvidia.com/gpugems/gpugems3/part-vi-gpu-computing/chapter-39-parallel-prefix-sum-scan-cuda>
 - [10] Sheng-Chun Kao, Suvinay Subramanian, Gaurav Agrawal, Amir Yazdanbakhsh, and Tushar Krishna. 2023. FLAT: An Optimized Dataflow for Mitigating Attention Bottlenecks. In *Proceedings of the 28th ACM International Conference on Architectural Support for Programming Languages and Operating Systems, Volume 2*. ACM, Vancouver BC Canada, 295–310. <https://doi.org/10.1145/3575693.3575747>
 - [11] Ben Keller, Rangharajan Venkatesan, Steve Dai, Stephen G. Tell, Brian Zimmer, William J. Dally, C. Thomas Gray, and Bruce Khailany. 2022. A 17–95.6 TOPS/W Deep Learning Inference Accelerator with Per-Vector Scaled 4-bit Quantization for Transformers in 5nm. In *2022 IEEE Symposium on VLSI Technology and Circuits (VLSI Technology and Circuits)*. IEEE, Honolulu, HI, USA, 16–17. <https://doi.org/10.1109/VLSITechnologyandCirc46769.2022.9830277>
 - [12] Sangyeob Kim, Sangjin Kim, Wooyoung Jo, Soyeon Kim, Seongyun Hong, and Hoi-Jun Yoo. 2024. 20.5 C-Transformer: A 2.6–18.1uJ/Token Homogeneous DNN-Transformer/Spiking-Transformer Processor with Big-Little Network and Implicit Weight Generation for Large Language Models. In *2024 IEEE International Solid-State Circuits Conference (ISSCC)*, Vol. 67. 368–370. <https://doi.org/10.1109/ISSCC49657.2024.10454330>
 - [13] Jinhao Li, Shan Huang, Jiaming Xu, Jun Liu, Li Ding, Ningyi Xu, and Guohao Dai. 2024. Mamba accelerator with reconfigurable architecture. *arXiv preprint arXiv:2409.11440* (2024).
 - [14] Yandong Luo and Shimeng Yu. 2024. H3D-Transformer: A Heterogeneous 3D (H3D) Computing Platform for Transformer Model Acceleration on Edge Devices. *ACM Transactions on Design Automation of Electronic Systems* (Feb. 2024), 3649219. <https://doi.org/10.1145/3649219>
 - [15] Eric Martin and Chris Cundy. 2018. Parallelizing Linear Recurrent Neural Nets Over Sequence Length. arXiv:1709.04057 [cs.NE] <https://arxiv.org/abs/1709.04057>
 - [16] Nandeeka Nayak, Xinrui Wu, Toluwanimi O. Odemuyiwa, Michael Pellauer, Joel S. Emer, and Christopher W. Fletcher. 2024. FuseMax: Leveraging Extended Einsums to Optimize Attention Accelerator Design. arXiv:2406.10491 [cs.AR] <https://arxiv.org/abs/2406.10491>
 - [17] ONNX Community. 2024. ONNX: Open Neural Network Exchange. <https://github.com/onnx/>.
 - [18] OpenAI. 2020. GPT-3: Language Models are Few-Shot Learners. <https://arxiv.org/abs/2005.14165>.
 - [19] Yubin Qin, Yang Wang, Dazheng Deng, Xiaolong Yang, Zhiren Zhao, Yang Zhou, Yuanqi Fan, Jingchuan Wei, Tianbao Chen, Leibo Liu, Shaojun Wei, Yang Hu, and Shouyi Yin. 2024. Ayaka: A Versatile Transformer Accelerator With Low-Rank Estimation and Heterogeneous Dataflow. *IEEE Journal of Solid-State Circuits* (2024), 1–15. <https://doi.org/10.1109/JSSC.2024.3397189>
 - [20] Yikan Qiu, Yufei Ma, Meng Wu, Yifan Jia, Xinyu Qu, Zecheng Zhou, Jincheng Lou, Tianyu Jia, Le Ye, and Ru Huang. 2024. Quartet: A 22nm 0.09mJ/Inference Digital Compute-in-Memory Versatile AI Accelerator with Heterogeneous Tensor Engines and Off-Chip-Less Dataflow. In *2024 IEEE Custom Integrated Circuits Conference (CICC)*. IEEE, Denver, CO, USA, 1–2. <https://doi.org/10.1109/CICC60959.2024.10529063>
 - [21] Arne Symons, Linyan Mei, Steven Colleman, Pouya Houshmand, Sebastian Karl, and Marian Verhelst. 2025. Stream: Design Space Exploration of Layer-Fused DNNs on Heterogeneous Dataflow Accelerators. *IEEE Trans. Comput.* 74, 1 (2025), 237–249. <https://doi.org/10.1109/TC.2024.3477938>
 - [22] Hugo Touvron, Louis Martin, Kevin Stone, Peter Albert, Amjad Almahairi, Yasmine Babaei, Nikolay Bashlykov, Soumya Batra, Prajwal Bhargava, Shrusti Bhosale, Dan Bikel, Lukas Blecher, Cristian Canton Ferrer, Moya Chen, Guillem Cucu-rull, David Esiobu, Jude Fernandes, Jeremy Fu, Wenyin Fu, Brian Fuller, Cynthia Gao, Vedanuj Goswami, Naman Goyal, Anthony Hartshorn, Saghar Hosseini, Rui Hou, Hakan Inan, Marcin Kardas, Viktor Kerkez, Madian Khabsa, Isabel Kloumann, Artem Korenev, Punit Singh Koura, Marie-Anne Lachaux, Thibaut Lavril, Jenya Lee, Diana Liskovich, Yinghai Lu, Yuning Mao, Xavier Martinet, Todor Mihaylov, Pushkar Mishra, Igor Molybog, Yixin Nie, Andrew Poulton, Jeremy Reizenstein, Rashi Rungta, Kalyan Saladi, Alan Schelten, Ruan Silva, Eric Michael Smith, Ranjan Subramanian, Xiaoqing Ellen Tan, Binh Tang, Ross Taylor, Adina Williams, Jian Xiang Kuan, Puxin Xu, Zheng Yan, Iliyan Zarov, Yuchen Zhang, Angela Fan, Melanie Kambadur, Sharan Narang, Aurelien Rodriguez, Robert Stojnic, Sergey Edunov, and Thomas Scialom. 2023. Llama 2: Open Foundation and Fine-Tuned Chat Models. arXiv:2307.09288 [cs.CL] <https://arxiv.org/abs/2307.09288>
 - [23] Ashish Vaswani, Noam Shazeer, Niki Parmar, Jakob Uszkoreit, Llion Jones, Aidan N Gomez, Lukasz Kaiser, and Illia Polosukhin. 2017. Attention is all you need. *Advances in neural information processing systems* 30 (2017).
 - [24] Samuel Williams, Andrew Waterman, and David Patterson. 2009. Roofline: an insightful visual performance model for multicore architectures. *Commun. ACM* 52, 4 (2009), 65–76.
 - [25] Shuai Yuan, Weifeng He, Zhenhua Zhu, Fangxin Liu, Zhuoran Song, Guohao Dai, Guanghui He, and Yanan Sun. 2024. HyCTor: A Hybrid CNN-Transformer Network Accelerator With Flexible Weight/Output Stationary Dataflow and Multi-Core Extension. *IEEE Transactions on Computer-Aided Design of Integrated Circuits and Systems* (2024), 1–1. <https://doi.org/10.1109/TCAD.2024.3490173>
 - [26] Susan Zhang, Stephen Roller, Naman Goyal, Mikel Artetxe, Moya Chen, Shuohui Chen, Christopher Dewan, Mona Diab, Xian Li, Xi Victoria Lin, et al. 2022. Opt: Open pre-trained transformer language models. *arXiv preprint arXiv:2205.01068* (2022).
 - [27] Susan Zhang, Stephen Roller, Naman Goyal, Mikel Artetxe, Moya Chen, Shuohui Chen, Christopher Dewan, Mona Diab, Xian Li, Xi Victoria Lin, Todor Mihaylov, Myle Ott, Sam Shleifer, Kurt Shuster, Daniel Simig, Punit Singh Koura, Anjali Sridhar, Tianlu Wang, and Luke Zettlemoyer. 2022. OPT: Open Pre-trained Transformer Language Models. arXiv:2205.01068 [cs.CL] <https://arxiv.org/abs/2205.01068>
 - [28] Gamze Islamoğlu, Moritz Scherer, Gianna Paulin, Tim Fischer, Victor J. B. Jung, Angelo Garofalo, and Luca Benini. 2023. ITA: An Energy-Efficient Attention and Softmax Accelerator for Quantized Transformers. (July 2023). arXiv:2307.03493 <http://arxiv.org/abs/2307.03493> arXiv:2307.03493 [cs].